

Numerical simulation of fish nets in currents using a Morison force model

Cristian Cifuentes¹ and M.H. Kim^{*2}

¹*Institute of Naval Architecture and Ocean Engineering Universidad Austral de Chile, Valdivia, Chile*

²*Department of Ocean Engineering Texas A&M University, College Station, TX, USA*

(Received April 17, 2017, Revised May 5, 2017, Accepted May 11, 2017)

Abstract. For complex flexible structures such as nets, the determination of drag forces and its deformation is a challenging task. The accurate prediction of loads on cages is one of the key steps in designing fish farm facilities. The basic physics with a simple cage, can be addressed by the use of experimental studies. However, to design more complex cage system for various environmental conditions, a reliable numerical simulation tool is essential. In this work, the current load on a cage is calculated using a Morison-force model applied at instantaneous positions of equivalent-net modeling. Variations of solidity ratio (S_n) of the net and current speed are considered. An equivalent array of cylinders is built to represent the physical netting. Based on the systematic comparisons between the published experimental data for Raschel nets and the current numerical simulations, carried out using the commercial software OrcaFlex, a new formulation for C_d values, used in the equivalent-net model, is presented. The similar approach can also be applied to other netting materials following the same procedure. In case of high solidity ratio and current speed, the hybrid model defines C_d as a function of Re (Reynolds number) and S_n to better represent the corresponding weak diffraction effects. Otherwise, the conventional C_d values depending only on Re can be used with including shielding effects for downstream elements. This new methodology significantly improves the agreement between numerical and experimental data.

Keywords: fish cage; equivalent net model; Morison drag formula; strong current; large deformation; solidity ratio; drag coefficient; weak diffraction effect; shielding effect

1. Introduction

As aquaculture keeps growing driven by the high demand for seafood around the globe, larger and more complex fish farms are being designed and installed in exposed locations. At these sites, continuous water exchange by waves and currents inside the cage and large external space provides ideal conditions for fish aquaculture (Cifuentes and Kim 2015). In these high energy seas, large deformations are expected on flexible nets. Since the deformation on the net is mainly driven by current loading, this has been the main focus of research over the last decade.

The wellbeing of the fish depends on the net internal volume while the force over the netting, induced mainly by current loading, drives the design of mooring elements. In addition, a large deformation can trigger interferences among cage components leading to structural failures.

*Corresponding author, Professor, E-mail: m-kim3@tamu.edu

To improve designs for various structural and environmental conditions, reliable numerical tools need to be developed handling intricate geometries and including nonlinear effects such as large deformations and viscous drag forces. In the present study, we have used the commercial software OrcaFlex to create an equivalent numerical net. This numerical tool uses a Morison force model to solve the dynamic responses of nets under current and wave actions. The main parameter in this force model is the drag coefficient C_d which depends on Reynolds number based on steady current speed and twine diameter. When using this approach, forces and deformations can be estimated with good precision for current speeds up to 0.5 m/s (Cifuentes and Kim 2015). However, at higher current velocities large deformations of the net occur and numerical results tend to deviate from experimental data even when shielding effect is included. This phenomenon happens especially when the net-solidity ratio is high.

Several experimental and numerical works have been carried out to predict drag forces over nets. Early experiments revealed the connection between drag load and net deformation (Aarnes and Løland 1990) and the reduction of fluid speed inside the cage, effect known as shielding effect (Løland 1993). Further experimental data quantified the reduction of internal volume on the cage as a function of current speed and ballast for a clean cylindrical net under mild current conditions (Lader and Enerhaug 2005). At high current speed, a flexible net pen shows a large volume reduction. In this condition, the increased blockage of the flow (or weak diffraction effect) leads to a reduction of the drag force when compared to less deformed conditions (Kristiansen *et al.* 2015). This is mainly due to the deflection of the flow below and around the cage (Gansel *et al.* 2012). This weak diffraction effect is even more significant for nets with high solidity ratios which experience changes on the direction of the flow even at mild current speeds (Moe-føre *et al.* 2014). Solidity ratio is defined as the ratio of the projected area of the net over the total area enclosed by the net (Klebert *et al.* 2013). Biofouling is another relevant factor when considering the blockage effect. For twine groups and simple net panels attached to rigid frames, an increase of S_n leads to an increase in drag forces when compared to clean nets (Lader *et al.* 2015, Swift *et al.* 2006).

In order to analyze more complex systems even including mooring/vessel/cage interaction (Cifuentes *et al.* 2014), numerical tools have been developed to predict the dynamic responses of nets under current and wave loading. The most common force models are based on screen type elements (Kristiansen and Faltinsen 2012) and Morison elements (Cifuentes and Kim 2015, Moe-Føre *et al.* 2015, Zhao *et al.* 2015). Both force models have been validated against experimental data using a bottomless cylindrical net, showing an over prediction of drag force at high current speed for large values of solidity ratio (Kristiansen and Faltinsen 2012). Discrepancies between numerical and experimental data are larger when using a Morison force model, even when wake effect is included in the numerical scheme (Cifuentes and Kim 2015). C_d values used on Morison equation must be determined for every type of netting material since there is a scatter due to the fabrication process and surface roughness on the thread of the net (Tsukrov *et al.* 2011). Multiple C_d formulations are available in the literature, each particular to the corresponding authors' frame of work (Klebert *et al.* 2013).

In this study, the net is represented by a group of cylinders and force is calculated based on the modified version of Morison equation (Haritos and He 1992) which accounts for instantaneous net positions and the relative velocity and acceleration between net element and current speed. The numerical model updates C_d values for the cylinders at each time step based on Reynolds number. Local wake effect is included by using Blevins formulation (Blevins 2005). The weak diffraction effects are considered in C_d when necessary. The numerical results, obtained using the present

methodology, are compared to published experimental data for a Raschel type of netting. The approach can straightforwardly be applied to other kinds of nets.

Nomenclature

S_n	Solidity Ratio
C_d	Drag Coefficient
Re	Reynolds number

2. Numerical model

A typical flexible cage considers three main components, the net to enclose the fish, an upper collar acting as buoyancy reserve and supporting the net, and a ballast system to preserve maximum volume of the net when exposed to currents.

Considering that it would be impractical to model every thread of the physical net, the present numerical representation is made such that a group of twines in the physical net are represented by an equivalent line element. In OrcaFlex, nets are modeled using a combination of lines and three-degree-of-freedom buoys. The interconnection of these elements creates an array of cylinders able to react to environmental loads as a single unit, while capturing the interaction between cage components. Lines are massless spring elements with two nodes at the end where mass, buoyancy, and drag forces are lumped (Orcina 2014).

Three-degree-of-freedom buoys are used as connections between lines, and they only transfer linear displacements, excluding rotations since bending stiffness of the net is considered negligible. These elements do not add drag or inertia forces to the system.

The surface collar is modeled dividing the circumference by 32 segments connected by six-degree-of-freedom buoys. These elements transfer rotations as well as linear displacements allowing the representation of bending stiffness. Mechanical and geometrical properties of the physical collar are assigned to the segments in the numerical model to capture its response under steady current load. For the ballast system in this particular analysis, an increase on the mass on specific buoys at the bottom of the net has been applied at the corresponding locations as in the prototype nets. The full description of those prototypes is given in the results section.

Two main parameters, projected area and wet weight (dry weight minus buoyancy), must be matched between numerical and physical nets. The diameter of the cylinders in the array representing the net in the numerical model is determined by the S_n value of the physical net and its total area. This procedure creates a numerical net heavier (Tsukrov *et al.* 2003) and stiffer (Fredheim 2005) than the physical net. Nonetheless, since mass and buoyancy properties of line and buoys are lumped into the end nodes, wet weight can be matched by modifying the buoyancy on the three-degree-of-freedom buoys connecting the line elements. To solve the problem of larger axial stiffness on the numerical net, the corresponding Young's modulus (E_m) is reduced following the procedure presented by Fredheim (2005) and described in Eq. (1).

$$E_m = E_p \frac{n_{tp} d_{tp}^2}{n_{tm} d_{tm}^2} \quad (1)$$

In the previous expression, m stands for model and p for prototype while d is twine (t) diameter. n_{tp} and n_{tm} characterize the number of twines contained in the same area in prototype and model nets respectively.

By discretizing the net using this methodology, a small number of elements are needed to estimate drag force and volume reduction. Previous studies confirm that increasing the number of elements used to describe the net does not have high influence over the accuracy of the results (Cifuentes and Kim 2015). In the present case, the model consists of 320 three-degree-of-freedom buoys and 672 lines in addition to 32 six-degree-of-freedom buoys used for the surface collar. Fig. 1 shows the numerical net including lines and buoys.

Drag and inertia forces over the equivalent net are calculated using Morison equation (Morison 1950), accounting for the relative velocity and acceleration between fluid and line elements (Haritos and He 1992) as presented in Eq. (2). Drag forces are obtained based on the cross flow principle to account for the angle of attack of the flow relative to the lines. The relative velocity is divided into components normal and parallel to the line axis. This axial load component is obtained using the drag load portion of Morison equation, considering the skin surface area defined as πdl , and C_t equal to 0.008.

$$F_w(t) = \frac{1}{2} \rho C_d dl [v(t) - u(t)] |v(t) - u(t)| + \rho C_M \frac{\pi}{4} d^2 l \dot{v}(t) - \rho (C_M - 1) \frac{\pi}{4} d^2 l \dot{u}(t) \quad (2)$$

In Eq. (2), $F_w(t)$ represents the fluid force, ρ is water density, d is element effective diameter, l is element length, C_M represents inertia coefficient and C_d stands for the drag coefficient in the normal direction relative to line axis, $u(t)$ and $v(t)$ are element and fluid velocities while $\dot{u}(t)$ and $\dot{v}(t)$ are element and fluid accelerations. This fluid force is applied to the instantaneous positions and inclinations of individual elements of the numerical net at each time step. The total force is the summation of the contribution from each element.

In Eq. (2), C_M is set equal to 2 and fixed during the simulation given that inertia loading is not significant for net elements (Lader *et al.* 2007). In OrcaFlex, C_d can be defined as a single constant value or a time dependent variable. In our model, C_d is determined at every time step based on the relative velocity between line element and fluid flow. The formulation given by DeCew *et al.* (2010) is implemented in the numerical model, calculating Re using Eq. (3). The angle of attack between line element and fluid velocity is considered into the calculation for Re .

$$Re_{flow} = \frac{|v_r| d \cos(\alpha)}{\nu} \quad (3)$$

$$v_r = v_{fluid} - v_{line}$$

In the previous expression ν represents kinematic viscosity and α the angle between the relative flow and the normal to the line's axial axis. Once Re is calculated, the corresponding C_d value is obtained according to Eq. (4) (DeCew and Tsukrov 2010).

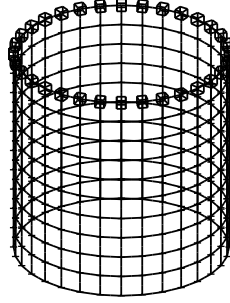


Fig. 1 Numerical model of the net

$$C_d = \begin{cases} \frac{8\pi}{Re * s} (1 - 0.87s^{-2}), & 0 < Re < 1 \\ 1.45 + 8.55Re^{-0.9}, & 1 < Re \leq 30 \\ 1.1 + 4Re^{-0.5}, & 30 < Re \leq 2.33 \times 10^5 \\ -3.41 \times 10^{-6} (Re - 5.78 \times 10^5), & 2.33 \times 10^5 < Re \leq 4.92 \times 10^5 \\ 0.401(1 - e^{-Re/5.99 \times 10^5}), & 4.92 \times 10^5 < Re \leq 10^7 \end{cases} \quad (4)$$

$$s = -0.077215655 + \ln(8 / Re)$$

Shielding effect can be included in the numerical model by using Blevins wake model which was derived for riser interactions (Blevins 2005). To apply the wake model, the cage is divided into two sections by a vertical plane perpendicular to the current direction. Upstream elements generate wake while downstream elements react to wake. This is illustrated in Fig. 2.

This simple model has been successfully implemented and validated by comparing numerical results with experimental data (Cifuentes and Kim 2015). Eqs. (5)-(7) describe the model. Drag and lift coefficients for downstream cylinders are calculated based on the distance, diameters, current speed, and drag coefficients of the upstream and downstream cylinders.

$$U(x, y) = U_0 \left(1 - 1.2 \left(\frac{C_{Duo} d_u}{x} \right)^{1/2} \right) \exp \left[\frac{-13y^2}{C_{Duo} d_u x} \right] \quad (5)$$

$$C_{Dd}(x, y) = C_{Ddo} \left(1 - a_1 \left(\frac{C_{Duo} d_u}{x} \right)^{1/2} m \right)^2 \quad (6)$$

$$C_{Ld}(x, y) = a_3 \left(\frac{y C_{Ddo} d_d}{x C_{Duo} d_u} \right) \left(\frac{C_{Duo} d_u}{x} \right)^{1/2} \left(1 - a_1 \left(\frac{C_{Duo} d_u}{x} \right)^{1/2} m \right) m \quad (7)$$

$$m = \exp \left[-\frac{a_2 y^2}{C_{Duo} d_u x} \right]$$

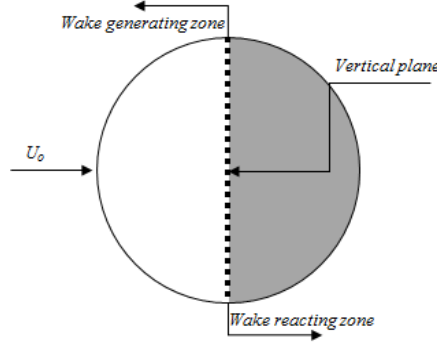


Fig. 2 Wake zone and vertical plane definition. U_o represents undisturbed current velocity

In Eqs. (5)-(7), (x,y) represents the coordinates of the downstream line with respect to the upstream element, C_{Dd} represents downstream cylinder drag coefficient calculated using undisturbed velocity U_o , C_{Ddo} is downstream cylinder drag coefficient based on reduced velocity $U(x,y)$, C_{Duo} upstream drag coefficient, d_u and d_d are upstream and downstream cylinder diameters, while C_{Ld} is the downstream element's lift coefficient. Parameters a_1 , a_2 and a_3 are constant values obtained after the formulation was fitted to experimental data. Their numerical values are 1.0, 4.5, and -10.6 respectively.

The positions (x,y,z) of the downstream elements are determined relative to the upstream elements. An element is in the wake region when the relative coordinate z is smaller than element length. Among those elements, the largest wake effect (largest velocity reduction) is selected and applied to the downstream line. A detailed explanation about this procedure can be found in Refs. (Cifuentes and Kim 2015, Blevins 2005).

The dynamic response of the system is solved at a local level first for each line element by using Eq. (8). This equation is solved by using an explicit forward Euler scheme with constant time step that calculates acceleration at the start of the time step (Orcina 2014). At each time step, the position of the elements is updated and the loads are applied at the instantaneous deformed net shape.

$$M(p,a) = F(p,v,t) - C(p,v) - K(p) \quad (8)$$

In Eq. (8), $M(p,a)$ is the local inertia load, $F(p,v,t)$ is the external load over the element, $C(p,v)$ is the element damping load and $K(p)$ is the stiffness load representing the effect of axial, torsional, and bending stiffness of the element. p,v,a and t are the position, velocity, acceleration, and time, respectively. The forcing component $F(p,v,t)$ includes $F_w(t)$ in addition to buoyancy and gravity forces. The global equation of motion for the system has the same form as the local one, except that it uses global loads and vectors. A ramping function is used to gradually apply loads over the system avoiding long transient effects. The described method is computationally efficient and achieves convergence faster using a small number of elements. The total simulation time ranges between 3 to 5 minutes for each current speed condition on an Intel®Core™ i7-3770 CPU@ 3.4 GHz processor with 32.0 GB installed RAM.

Table 1 Netting characteristics

Solidity ratio S_n	Half mesh (mm)	Twine diameter (mm)
0.1904	25.5	2.60
0.2250	16.0	1.80
0.3020	16.2	2.66
0.4340	5.8	1.35

3. Results and discussions

Using the previously described numerical procedure, calculations were performed to compare with the experimental data published by Lader and Enerhaug (2005) and Moe-Føre *et al.* (2014). In both works, a Raschel type net was used to build a cylindrical cage open at top and bottom. A simple ballast system, including point masses at 16 points along the bottom of the cage was used. In these experiments, the surface collar is treated as a rigid body. The drag over the net was isolated by extracting the drag force of the upper collar and ballast cylinders from the total drag force.

In the case of the experiment by Lader and Enerhaug (2005), the net pen has a diameter of 1.435 m., draft of 1.44 m, and S_n equal to 0.2250. The density of the net is 1130 kg/m³. For ballast, 16 point masses of 400 gr. each were hanging from the bottom perimeter of the net pen. On the experiments by Moe-Føre *et al.* (2014), three nets with S_n values of 0.1904, 0.3020, and 0.4340 were tested. The diameter of the cage in this case is 1.75 m. and draft 1.5 m. Net density is 1100 kg/m³ and ballast is applied at 16 points along the circumference of the net bottom with a wet weight of 4.48 N. The Young's modulus of the net material was not given as part of the experimental data. Therefore, a value of 8.10×10^7 Pa is used for all the studied nets, which corresponds to the average value for wet Raschel nets (Moe *et al.* 2007, DeCew *et al.* 2013).

The description of the netting geometry is presented in Table 1. For S_n equal to 0.1904 and 0.3020, the diameter of the twine has been modified from the original physical value to account for the projected area of knots connecting the twines.

The four cages tested in this analysis were subjected to current speed varying from 0.03 to 0.93 m/s. For each case, current speed is considered constant over water depth. For the case of S_n equal to 0.2250, the maximum current speed for calculations is 0.52 m/s. Fig. 3 shows the large deformation of the net for S_n equal to 0.3020 under 0.5 m/s current speed. The deformed shapes are similar.

Calculations with and without including shielding effect were carried out to demonstrate the performance of the numerical models for the drag force on the cage. The comparison of the numerical and experimental results using the formulation given by DeCew *et al.* (2010) for C_d and Blevins wake model are presented in Fig. 4.

In general, numerical calculations show good agreement with experiments over a wide range of current speed, especially for S_n values of 0.1904 and 0.225. For higher solidities, good agreement is reached for current speeds up to 0.5 m/s. The inclusion of the wake model gives slightly smaller drag forces, which better correlates with the experimental data.

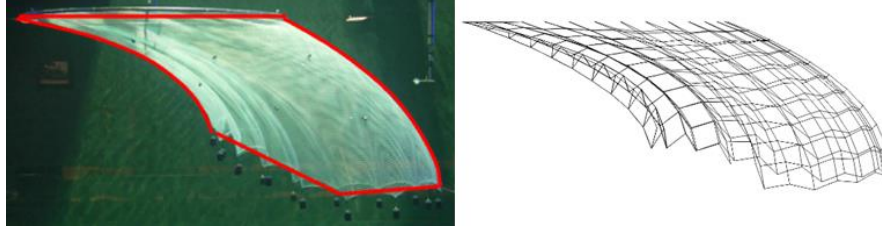


Fig. 3 Net deformation from experiments (Moe-Føre *et al.* 2015) and numerical calculations

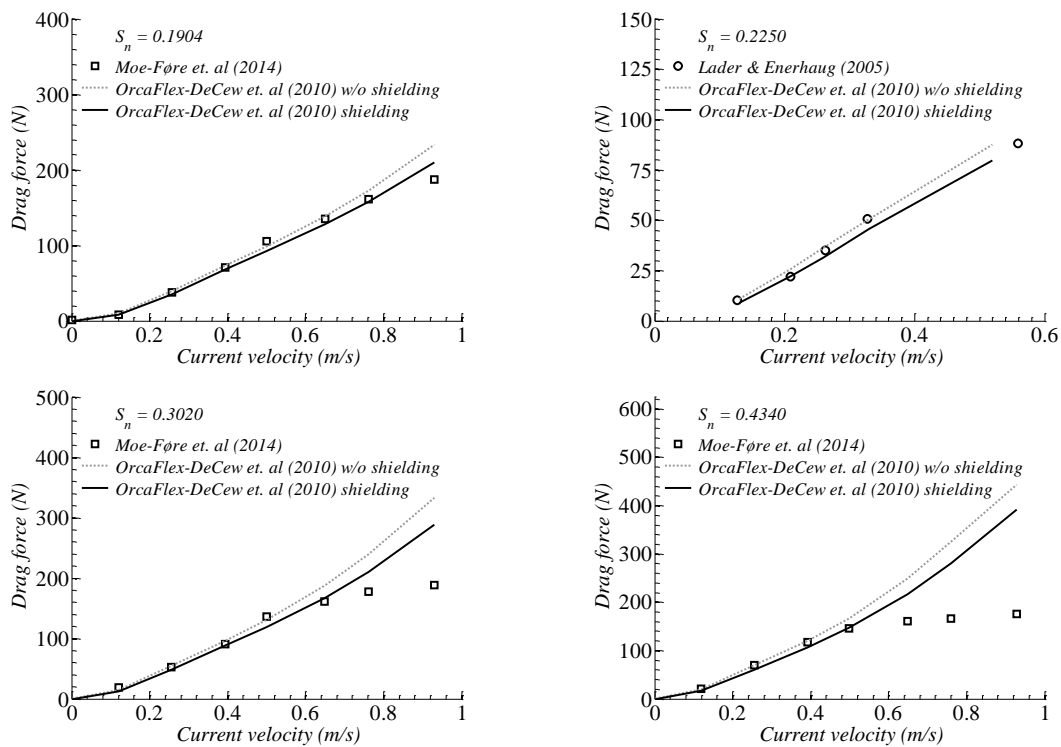


Fig. 4 Comparison of numerical and experimental results for drag force under steady current

Fig. 4 shows that for high current speed and high solidity ratio, the differences between numerical calculations and experimental data become substantial. The main reason for this effect is the flow redirection and increased blockage when the net of high solidity ratio is largely deformed. For high-solidity nets with large deformation, the flow goes around and below the net instead of flowing through it. This phenomenon is translated into the plateau of the drag force versus current speed curves for current speed larger than 0.5 m/s and solidity ratio higher than 0.3. The change of flow direction (or weak diffraction effect) cannot be directly modeled in the present numerical scheme. On the other hand, when necessary, the blockage effect can indirectly be considered by modifying the drag coefficient formula for the constituent elements of the numerical net since the

C_d formulation by DeCew *et al.* (2010) cannot directly be used under high current speeds and high solidity ratio. Accordingly, C_d , based on twine diameter and including shielding effect, needs to be adjusted based on experimental drag force data.

Numerical calculations show that drag coefficient values for nets of high solidity ratios, at high current speed, must be smaller than those from Eq. (4), which reflects the effect of weak diffraction, as described earlier (Gansel *et al.* 2012). This global effect can indirectly be included in our numerical model by the adequate definition of drag coefficients for such conditions.

Since the determination of drag coefficient in this numerical scheme is based on twine diameter, a third source of experimental data can directly be added to the study. In the research performed by Tsukrov *et al.* (2011), several nets were characterized in terms of drag coefficients by experimental measurements. Net panels were exposed to current speed ranging from 0.1 to 1.0 m/s. In particular, two Raschel type nets were included in Tsukrov *et al.* (2011) considering S_n values of 0.172 and 0.208.

C_d as a function of Re for all the data, including experimental and numerical sources, is presented in Fig. 5. Additionally, the values for C_d given by Eq. (4) are included for comparison, which correlates reasonably with the experimental data except those 5 points. Those five points marked by + were obtained so that the current numerical simulation can generate the same drag force on the net as the measurement. No clear trend is observed in relating the drag coefficients of those cases as a function of Re only since those five points reflect the additional effects of weak diffraction with the large deformation of high-solidity-ratio net in strong current.

To better represent the weak diffraction effect for high solidity ratio and high current speed, instead of presenting drag coefficient as a function of Re only, C_d is represented by a new variable $Re * S_n^2$. Then, a better trend can be observed as shown in Fig. 6. This trend is interesting given that the plot is made using four different sources of data, covering a wide range of current velocities and solidity ratios. This approach is intended to be valid for nylon Raschel nets, while for other types of nets, the relevant physics is to be similar and a similar approach can be used to better characterize the variation of C_d across different net opening geometries and fluid regimes.

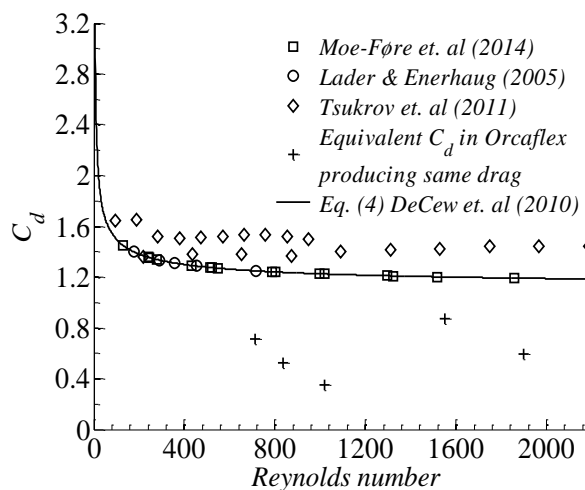


Fig. 5 C_d as a function of Re based on experimental and numerical data

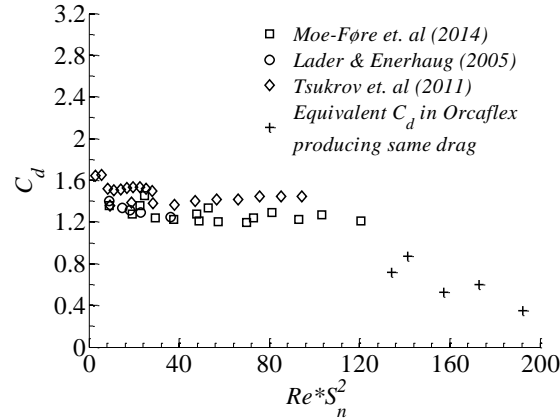


Fig. 6 C_d as a function of Re and S_n

In the region defined by $Re * S_n^2 < 110$ in Fig. 6, the numerical results using the formulation by DeCew *et al.* (2010) including the wake model by Blevins, show good agreement with experimental data. In this region, the drag coefficients slightly scatter with a mean of 1.4, which is the characteristic C_d value for smooth cylinders in subcritical flow (Sumer and Fredsoe 1997). For $Re * S_n^2 > 110$, C_d values decrease rapidly. This region represents the weak diffraction effect due to the large deformation of the net. In the physical net, both change of flow direction, reduction of net effective porosity due to large deformation, and reduction of current velocity downstream contribute to the phenomenon. The phenomenon can be described in the present numerical model by the reduction of C_d values of the net.

The region of interest in Fig. 6 where $Re * S_n^2 > 110$, can be described by a polynomial fit of the data using the least-square method. In this manner, a new formulation for C_d values is found for Raschel nets in the blockage conditions.

The new combined expression for C_d based on the factor $Re * S_n^2$ can be described as in Eq. (9).

$$\text{Use Eq.(4) including shielding effect for } Re * S_n^2 < 110 \quad (9)$$

$$C_d = 1.7451 - 0.0071 * (Re * S_n^2) \quad \text{for } Re * S_n^2 > 110$$

This new formulation is implemented into the present numerical model by OrcaFlex and the drag force calculations in Fig. 4 are revised. The results are given in Fig. 7.

The overall comparison, especially for those cases of weak-diffraction regime, is significantly improved. When compared to Fig. 4, the maximum error is reduced from 120% to 10% for the case of S_n equal to 0.4340. The results show that a proper modification of C_d values is a viable alternative to represent the complex physics related to the weak-diffraction effect. Most importantly, it is a simple and efficient manner when the Morison force model is used for the simulation of nets. This analysis also illustrates how the same approach can be applied to other nets when using the Morison force model.

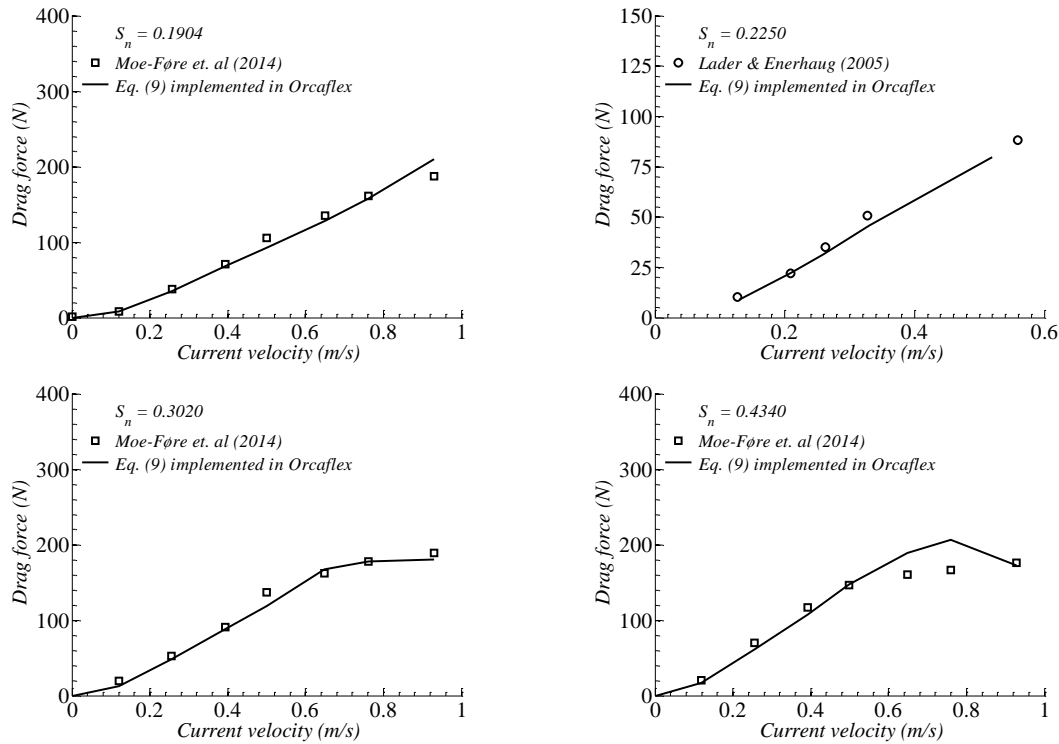


Fig. 7 Comparisons of numerical and experimental results for drag forces under steady current using new C_d definition

As seen from the calculations presented in this work, a Morison force model is not able to accurately predict forces when flow is deflected due to the large deformation of the netting. Recent experimental data have confirmed the redirection of the flow underneath and around cylindrical cages for solidity ratios above 0.3 (Turner and Reid 2015). This change of speed and direction of the flow cannot be described in the current Morison-formula-based numerical model using C_d solely a function of Re .

CFD calculations have revealed the complex flow pattern in the wake of a single net panel (Bi *et al.* 2014) as well as on rigid porous cylinders (Gansel *et al.* 2012). Even for these simple net models, the computational time required to obtain the results is quite large and thus not practical for finding the optimal design by repeated simulations, especially for multiple cages. On the other hand, a simple model as the one presented in this analysis, is able to converge in a short time using a small number of elements to discretize the net. In addition, for further analysis including waves, the same approach can be used.

The determination of drag forces over nets with high solidity ratios is particularly interesting for fish farms exposed to high levels of biofouling. Recent studies have shown that the levels of biofouling can be parametrized in order to use the existent method of calculation of forces over nets (Gansel *et al.* 2015). By using Eq. (9), calculations can be done to reasonably determine the drag loads over fish farms after being installed, and using this information, the schedule of

cleaning or replacement of nets can be made. This kind of reliable prediction of forces on bio-fouled nets can also help to avoid failures of the cage system.

4. Conclusions

A new formulation for the determination of C_d values for Raschel nets have been developed using a combination of available published experimental data and numerical simulations. The formulation is based on the flow regime by Re , considering twine diameter, and net geometry based on S_n . On the numerical model, the shielding effect of the upstream portion of the net over the elements downstream has also been included.

The drag forces on the nets are well captured by using the conventional C_d and Morison formula applied at instantaneous equivalent-net-element position for current speed less than 0.5 m/s and S_n values up to 0.3. The inclusion of shielding effects slightly improves the comparisons against measurement data. For higher solidity ratio and current velocity, the weak diffraction effects can happen and they can more reasonably be simulated by using the new approach i.e. C_d is a function of both Re and S_n , with which better agreement is achieved between the numerical and experimental data than the C_d formulation based solely on Reynolds number. The newly suggested combined formulas prove to be adequate for a wide range of netting solidity ratios and current speeds. The methodology presented to characterize the net in terms of drag coefficient can directly be applied to the case including waves. It can also be applied to other types of nets, for which further laboratory tests are required.

References

- Aarnes, J.V. and Loland, G. (1990), "Current forces on cage, net deflection", *Eng. Offshore Fish Farm.*, 137-152.
- Bi, C.W., Zhao, Y.P., Dong, G.H., Xu, T.J. and Gui, F.K. (2014), "Numerical simulation of the interaction between flow and flexible nets", *J. Fluids Struct.*, **45**, 180-201.
- Cifuentes, C. and Kim, M.H. (2015), "Dynamic analysis for the global performance of an SPM-feeder-cage system under waves and currents", *China Ocean Eng.*, **29**(3), 415-430.
- Cifuentes, C. and Kim, M.H. (2015), "Numerical simulation of wake effect in nets under steady current", *Proceedings of the ASME 2015 34th International Conference on Ocean, Offshore and Arctic Engineering OMAE2015*.
- Cifuentes, C., Kim, M.H., Sims, N.A. and Key, G. (2014), "Coupled analysis of a SPM Buoy- Feeder- Cage system for offshore aquaculture", *Proceedings of the 24th International Ocean and Polar Engineering Conference*.
- DeCew, J., Fredriksson, D.W., Lader, P. F., Chambers, M., Howell, W.H., Osienki, M., Celikkol, B., Frank, K. and Høy, E. (2013), "Field measurements of cage deformation using acoustic sensors", *Aquacult. Eng.*, **57**, 114-125.
- DeCew, J., Tsukrov, I., Risso, A., Swift, M.R. and Celikkol, B. (2010), "Modeling of dynamic behavior of a single-point moored submersible fish cage under currents", *Aquacult. Eng.*, **43**(2), 38-45.
- Fredheim, A. (2005), "Current forces on net structures", Norwegian University of Science and Technology, PhD Thesis.
- Gansel, L.C., McClimans, T.A. and Myrhaug, D. (2012), "Average flow inside and around fish cages with and without fouling in a uniform flow", *J. Offshore Mech. Arct.*, **134**, 41201.

- Gansel, L.C., Plew, D.R., Endresen, P.C., Olsen, A.I., Misimi, E., Guenther, J. and Jensen, Ø. “Drag of Clean and Fouled Net Panels – Measurements and Parameter
- Haritos, N. and He, D.T. (1992), “Modelling the response of cable elements in an ocean environment”, *Finite Elem. Anal. Des.*, **11**, 19-32.
- Klebert, P., Lader, P., Gansel, L. and Oppedal, F. (2013), “Hydrodynamic interactions on net panel and aquaculture fish cages: A review”, *Ocean Eng.*, **58**, 260-274.
- Kristiansen, D., Lader, P., Jensen, Ø. and Fredriksson, D. (2015), “Experimental study of an aquaculture net cage in waves and current”, *China Ocean Eng.*, **29**(3), 325-340.
- Kristiansen, T. and Faltinsen, O.M. (2012), “Modelling of current loads on aquaculture net cages”, *J. Fluids Struct.*, **34**, 218-235.
- Lader, P., Fredriksson, D.W., Guenther, J., Volent, Z., Blocher, N., Kristiansen, D., Gansel, L. and DeCew, J. (2015), “Drag on hydro-fouled nets -An experimental approach”, *China Ocean Eng.*, **29**(3), 369-389.
- Lader, P., Jensen, A., Sveen, J.K., Fredheim, A., Enerhaug, B. and Fredriksson, D. (2007), “Experimental investigation of wave forces on net structures”, *Appl. Ocean Res.*, **29**, 112-127.
- Lader, P.F. and Enerhaug, B. (2005), “Experimental investigation of forces and geometry of a net cage in uniform flow”, *IEEE J. Ocean. Eng.*, **30**(1), 79-84.
- Løland, G. (1993), “Current forces on, and flow through and around, floating fish farms”, *Aquacult. Int.*, **1**, 72-89.
- Moe-Føre, H., Christian Endresen, P., Gunnar Aarsæther, K., Jensen, J., Føre, M., Kristiansen, D., Fredheim, A., Lader, P. and Reite, K.J. (2015), “Structural analysis of aquaculture nets: Comparison and validation of different numerical modeling approaches”, *J. Offshore Mech. Arct.*, **137**(4), 41201.
- Moe-føre, H., Endresen, P.C., Aarsæther, K.G., Jensen, J., Føre, M., Kristiansen, D., Fredheim, A., Lader, P. and Reite, K. (2014), “Structural analysis of aquaculture nets: comparison and validation of different numerical modelling approaches”, *Proceedings of the ASME 2014 33rd International Conference on Ocean, Offshore and Arctic Engineering OMAE2014*.
- Moe, H., Olsen, A., Hopperstad, O.S., Jensen, Ø. and Fredheim, A. (2007), “Tensile properties for netting materials used in aquaculture net cages”, *Aquacult. Eng.*, **37**, 252-265.
- Morison, J.R., Johnson, J.W. and Schaaf, S.A. (1950), “The force exerted by surface waves on piles”, *J. Pet. Technol.*, **2**, 149-154.
- Orcina (2014), *OrcaFlex Manual Version 9.8a*. Ulverston, Orcina.
- R. D. Blevins, “Forces on and Stability of a Cylinder in a Wake,” *J. Offshore Mech. Arct.*, **127**, 39.
- Sumer, B.M. and Fredsoe, J. (1997), *Hydrodynamics around cylindrical structures*. Singapore: World Scientific Publishing Company.
- Swift, M.R., Fredriksson, D.W., Unrein, A., Fullerton, B., Patursson, O. and Baldwin, K. (2006), “Drag force acting on biofouled net panels”, *Aquacult. Eng.*, **35**, 292-299.
- Tsukrov, I., Drach, A., DeCew, J., Robinson Swift, M. and Celikkol, B. (2011), “Characterization of geometry and normal drag coefficients of copper nets”, *Ocean Eng.*, **38**(17-18), 1979-1988.
- Tsukrov, I., Eroshkin, O., Fredriksson, D., Swift, M.R. and Celikkol, B. (2003), “Finite element modeling of net panels using a consistent net element”, *Ocean Eng.*, **30**, 251-270.
- Turner, A.A. and Reid, G.K. (2015), “Experimental investigation of fish farm hydrodynamic properties on 1:15 scale model circular aquaculture cages”, *Proceedings of the ASME 2015 34th International Conference on Ocean, Offshore and Arctic Engineering OMAE2015*.
- Zhao, Y.P., Wang, X., DeCew, J., Tsukrov, I., Bai, X.D. and Bi, C. (2015), “Comparative study of two approaches to model the offshore fish cages”, *China Ocean Eng.*, **29**(3), 459-472.